2020 IEEE Conference on Control Technology and Applications (CCTA)
August 24-26, 2020. Montréal, Canada

Development of a spraying robot for precision agriculture: An edge following approach

Adrien Danton[1] and Jean-Christophe Roux[1] and Benoit Dance[2] and Christophe Cariou[1] and Roland Lenain[1]

Abstract— **This paper proposes several contributions to the development of an agricultural robot performing spraying task autonomously, in the framework of vineyard or orchard. Since an important point of such an application relies on the treatment of the vegetation while reducing the dissemination of hazardous chemical products, a control approach related to the detection of plants using Lidar is proposed for both controlling the robot motion and achieving spraying automation. A dedicated spraying device, allowing to (de)activate independently several nozzles has been designed and on-boarded on a mobile robot, following autonomously a detected structure (typically a row of trees). The synchronization of the sprayer and the robot with respect to the vegetation is ensured through an anticipative approach allowing to apply spraying on the vegetation pending on the robot motion.**

I. INTRODUCTION

The increasing worldwide population requires to maintain a high level of food production, while reducing the environmental impact of human activities. This is particularly the case in the field of agriculture [1]. As a result, it is mandatory to propose new solutions able to be environmental friendly, such as Precision Agriculture [2]. Nevertheless, such principles require to develop new technologies enabling to apply such approaches, without requiring a painful, and sometimes hazardous manpower. In such a context, the use of robots in agriculture arises as a promising solution [3], allowing to achieve a repetitive work, without losing accuracy along the working day. Such a field of application is more and more popular in robotics research and several robots are nowadays marketed [4].

The use of robots for Precision Farming is particularly important for spraying applications. The spraying task indeed uses a big amount of chemical products, which have important impacts on environment and may be hazardous for human. If some devices have been developed to optimize spraying (from planning [5] up to the automation of implements [6]), they still require the use of a human driving, implying potential interaction with products and to move at important speeds, without adaptation to the vegetation covering. First robots considering spraying (such as presented in [7]), are also developed, but are not necessarily designed to adapt spraying with respect to the vegetation, or are not appropriate to operate in vineyard or orchard.

In this paper, an autonomous robot on-boarding an automated spraying device with several independent nozzles mounted on a vertical ramp, is proposed to achieve autonomously a spraying task, adapting to the vegetation coverage. Despite the design of the mobile robot is generic and may embed several kinds of sensors (GPS, IMU, cameras, ...), this paper is focused on a spraying application in vineyard or orchard, for which the interaction with trees are predominant. As a result, the robot control is based on a relative perception with respect to the row of vegetation relying on an horizontal Lidar for robot guidance, and a vertical Lidar for leaves detection, with the aim of optimizing spraying. Based on this material, a control architecture is proposed. It is based on an edge detection approach [8], to ensure an accurate relative positioning of the sprayer with respect to the vegetation. In parallel, the estimation of the vegetation covering [9] is achieved thanks to the vertical lidar, settled in front of the robot. This permits to anticipate for the delay in the nozzles cut-off and optimize the efficiency of spraying with respect to the vegetation coverage, thanks to several independent nozzles.

This paper is decomposed as follows. First, the spraying robot with the on-boarded sensors and actuators is described, as well as the design of the spraying tool, allowing to specify the background and assumptions. The control of each part of the robot (motion and spraying) is detailed in a second part, describing in particular the synchronization between the robot motion and the implement actuation. Experimental results are then proposed in a third part, allowing to evaluate the effectiveness of the proposed architecture. Finally a last section concludes the paper and proposes future works.

II. AUTONOMOUS SPRAYING ROBOT DESCRIPTION

A. Mobile robot

This paper aims at developing a robot able to achieve autonomous and optimized spraying in rows of a relatively high vegetation, such as in vineyard and orchard. As rows may be relatively narrow, the robot depicted on the figure 1 has been designed with a configurable track (defined in the picture as its minimal length of $0.7m$). It is propelled electrically and is four-wheeled driven and steered, thanks to four independent wheeled-motors and four independent steering actuators. The wheelbase is set to $1.38m$, for a total length of $2m$, and weights $550Kg$ (for a maximal payload of $150Kg$). It is able to climb slopes up to $15°$, and reach

[1]these authors are with Université Clermont Auvergne, INRAE, UR TSCF, 63178, Aubiere, France firstname.lastname@inrae.fr
[2]Benoit Dance is with the Estia Institute of Technologies, Technopole Izarbel, 64210 Bidart, France benoit2702@hotmail.fr

speeds up to $10m.s^{-1}$ (in the wide track configuration, i.e. $1.3m$).

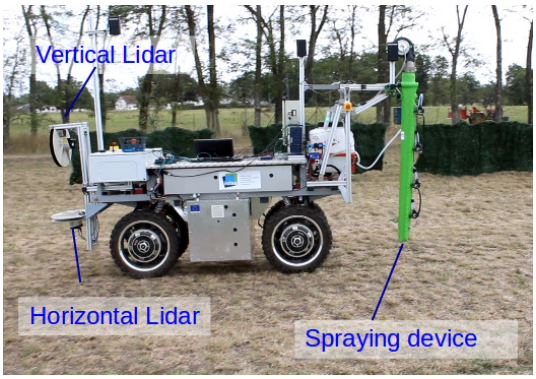

Fig. 1. The developed robot for autonomous spraying

Such a robot is used for research purpose and may be equipped with different sensors to achieved different kinds of tasks. For the purpose of autonomous spraying, two main sensors are used. A first Lidar, with a field of view of 270° is settled horizontally in front of the robot. It is dedicated to the detection of rows for autonomous guidance. A second Lidar is also settled in front of the robot but vertically, in order to detect the presence of vegetation in front of the nozzles of the sprayer device.

B. Edge detection

As has been mentioned previously, the motion of the robot is achieved with respect to the rows of plantation. These rows are detected thanks to the horizontal Lidar, which supplies a point cloud in the plan of the sensor. The objective is to derive from this point cloud, an edge which can be followed by the robot on one side of the robot with an offset.

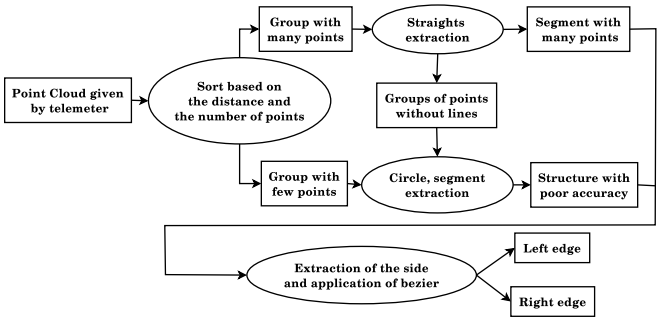

Fig. 2. Algorithm to estimate surrounding structures.

The computation of the edge from the cloud of points is achieved by the algorithm detailed on the figure 2. It relies on a geometry computation such as in [10]. Nevertheless, in this latter works, only the indoor segment detection is considered. This method is then not suitable for agricultural context. Consequently, an extension of this method to segment and curve detections is here proposed, based on the following steps:

- **Group of points.** From the point cloud given by the Lidar, it is relevant to distinguish types of points. First, the nearest points are gathered using a preliminary defined threshold [11]. After this first division, a second algorithm sorts these groups points in categories of interest pending on the group size.
- **Estimation of surrounding structures.** Each relevant group previously obtained and classified is differently processed in function of its size. An incremental algorithm [12] based on Least Median Square (LMS) (similar to Line-Tracking) is used to extract best straights from the big group [13]. If directions of several estimated straight lines in a row are nearly the same, then these subgroups are merged into a same group to define a segment. To avoid curvature discontinuity, it has been chosen to use Bezier curves to link each segment of a same group. On groups of points with a medium size, another incremental algorithm based on LMS method is used.
- **Trajectory computation.** From previous points generation, two local trajectories are then computed (right and left if available). To achieve this, a second order trajectory is computed from a least square method from the points classified on the left and on the right of the laser.

This algorithm allows obtaining at least one smooth and stable trajectory to follow with respect to the detected edge, robust with respect to dust and light perturbations. Based on this trajectory, one can easily compute the lateral and angular deviations of the robot, which constitute the robot state, such as detailed in the section III-A.

C. Spraying device and sensor

In order to achieve an accurate spraying only on the vegetation, a sprayer device has been designed and mounted at the rear of the robot (see figure 1). It is composed of four independent nozzles. Each of them are equipped with a solenoid valve, allowing to differentiate several areas for spraying. A tank of 50L, associated to a controllable pump is settled on the back of the robot in order to regulate the pressure inside the sprayer ramp. A global controller, operated thanks to a can bus has been developed to manage autonomously the elements of the sprayer:

- the four solenoid valves corresponding to the nozzles
- the flow in the spraying ramp
- the control mode (manual/autonomous)

In order to permit a common framework with the mobile robot, a ROS interface has been designed, allowing to proceed in the same algorithm, the control of both motion and spraying.

III. Motion control

A. Motion model

In this paper, the objective of motion control consists in following a structure, detected with a laser scanner. For that purpose, a control strategy based on the trajectory tracking point of view is considered here, as classically investigated in [14]. In this point of view, an ackerman-steering robot can

be described as a bicycle such as depicted on the figure 3. The robot is reduced to two wheels, one for the front axle with a steering angle denoted as δ^F, and one for the rear axle. The trajectory to be followed Γ is computed thanks to

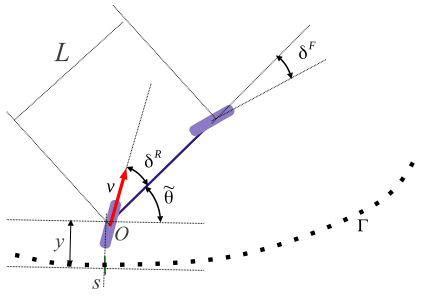

Fig. 3. Modelling of the mobile robot w.r.t. the detected structure Γ.

the edge detection algorithm described in the section II-B, which permits to measure the lateral and angular deviations, which constitute the state to be controlled:

$$X = \begin{bmatrix} y \\ \tilde{\theta} \end{bmatrix} \tag{1}$$

The position of the robot is indeed defined with respect to the detected structure, with a lateral error y at the curvilinear abscissa s, to be regulated to a desired set point y^d, thanks to the steering angle δ^F. The edge detection also permits to compute the local curvature of the edge $c(s)$. In this paper, the control of the velocity v of the robot is not considered, and this variable is then viewed as a known parameter. Using these notations, the classical motion model may be defined as (see [14] for details):

$$\dot{X} = \begin{bmatrix} \dot{y} &=& v\sin(\tilde{\theta}+\delta^R) \\ \dot{\tilde{\theta}} &=& v\frac{\tan\delta^F}{L} - \frac{c(s)\,v\cos(\tilde{\theta}+\delta^R)}{1-y\,c(s)} \end{bmatrix}. \tag{2}$$

with L the wheelbase of the robot. Using these notations the aim of the motion control is to derive an expression for the steering angle δ^F, ensuring the regulation of the lateral error y to some desired set point y^d.

B. Reactive steering angle control law

Thanks to the model (2), one can compute a control law for the front steering angle to follow the detected edge at a desired distance. This approach is based on the algorithm proposed in [15], here adapted to an Ackermann robot. Let us consider the tracking error e_y, such as:

$$e_y = y - y^d \ , \tag{3}$$

Considering that the achieved distance along the detected edge s may be derived with respect to time as:

$$\dot{s} = \frac{v\cos\tilde{\theta}}{1-c(s)y} \ , \tag{4}$$

one can derive the error defined by (3) with respect to the achieved distance by :

$$e'_y = \alpha\tan(\tilde{\theta}) \ , \tag{5}$$

with $\alpha = (1-y\,c(s))$. Let us consider $\tilde{\theta}$ as an intermediate control variable. One can note that if we impose for this variable, the expression (6),

$$\tilde{\theta}_d = \arctan\left(\frac{k_y e_y}{\alpha}\right) \ , \tag{6}$$

the dynamic of the error (5) becomes:

$$e'_y = k_y\,e_y \ , \tag{7}$$

where k_y is a negative scalar that regulates the settling distance of the convergence of the lateral deviation of the robot to the desired lateral deviation y_d. The virtual control value (6) of θ_d then constitutes a set point to be reached by the apparent orientation of the robot to ensures the objective.

Based on this consideration, the steering angle has now to be controlled in order to ensure the convergence of $\tilde{\theta}$ to $\tilde{\theta}_d$. To reach this goal, let us consider the second error $e'_{\tilde{\theta}} = \tilde{\theta} - \tilde{\theta}_d$. Thanks to the model (2), the derivative of this error with respect to the achieved distance may be written as:

$$e'_{\tilde{\theta}} = \alpha\frac{\tan(\delta^F)}{L\cos(\tilde{\theta})} - c(s) \ . \tag{8}$$

Providing that $\tilde{\theta}_d$ is slow-varying w.r.t. the achieved distance ($\tilde{\theta}'_d \approx 0$) compared to the yaw dynamics imposed to the robot, the convergence of this error to zero may then be imposed considering the control law (9) for the front steering angle such that:

$$\delta^F = \arctan\left(\frac{L\cos(\tilde{\theta})}{\alpha}\left(k_{\tilde{\theta}}e_{\tilde{\theta}} + c(s)\right)\right) \ . \tag{9}$$

The control law (9) indeed leads to the following expression for the error dynamics:

$$e'_{\tilde{\theta}} = k_{\tilde{\theta}}\,e_{\tilde{\theta}} \ , \tag{10}$$

where $k_{\tilde{\theta}}$ is a negative scalar that regulates the convergence of $e_{\tilde{\theta}}$ to zero under a settling distance. This gain defines a settling distance, and has to be chosen to ensure a faster convergence than the one imposed to the error related to the lateral deviation e_y. As a result, the following criterion $k_{\tilde{\theta}} \gg k_y$ has to be satisfied. The advantage of the propose approach first lies in the consideration of the derivative with respect to achieved distance. This permits to avoid the singularity classically appearing when the robot stops ($v = 0$).

C. Angular deviation limitation

A second interest of the backstepping approach is the intermediate control of the relative orientation of the robot, particularly attractive to avoid any contact of the robot with respect to the structure to be followed. One can indeed see on the figure 4, that when regulating a desired lateral distance, the front of the robot may touch the structure, when important curvature are observed.

In such configuration, in order to avoid collisions, the robot must turn despite the correct regulation of the error. In order to avoid this kind of situation, it is possible to compute the minimal admissible orientation of the robot to avoid the

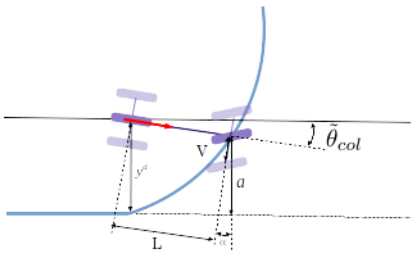

Fig. 4. Case of collision while the robot is well regulated.

collision. This angle, denoted $\tilde{\theta}_{col}$, may be geometrically defined by:

$$\tilde{\theta}_{col} = \arcsin\left(\frac{y-T-a}{L}\right) , \quad (11)$$

with T the half-track of the robot, and a the distance between the tangent at the trajectory and the impact point. If we consider that the trajectory is locally circular (such as suggested on the figure 4), with a radius of $\frac{1}{c(s)}$, this distance a may be approximated by the following expression:

$$a = \frac{1-\cos\gamma}{c(s)} , \quad (12)$$

with $\gamma = \arctan(Lc(s))$. The expression (11) exists under the conditions $|\frac{y-V-a}{L}| < 1$, which means that the front of the robot stays bellow the structure, which is assumed to be the case in practice. Since the structure to be followed can be located on the right or on the left of the robot, $\tilde{\theta}_{col}$ has two possible values denoted $\tilde{\theta}_{col_{right}}$ and $\tilde{\theta}_{col_{left}}$, depending on the side where the structure is. As soon as these two limits are known, an advantage of the proposed backstepping approach lies in the fact that the desired apparent orientation of the robot $\tilde{\theta}_d$, computed by the control law (6) can be bounded. In the following, these limits are computed in real time and the targeted apparent orientation is defined such as:

$$\tilde{\theta} = \begin{cases} \xi & \text{if } \tilde{\theta}_{col_{right}} < \xi < \tilde{\theta}_{col_{left}}, \\ \tilde{\theta}_{col_{left}} & \text{if } \xi > \tilde{\theta}_{col_{left}}, \\ \tilde{\theta}_{col_{right}} & \text{if } \xi < \tilde{\theta}_{col_{right}}, \end{cases} \quad (13)$$

with $\xi = \arctan\left(\frac{k_y e_y}{\alpha}\right)$, such as defined by (6).

IV. Sprayer control

A. Vegetation detection

Within the framework of our objective (i.e. the automation of the activation of the spraying devices according to the plant covering), the first step for sprayer control consists in perceiving the presence or absence of the vegetation in front of the nozzles. In order to account for the delay between the control signal sent to the solenoid and the actual opening/closing of the nozzle, the detection is achieved thanks to a vertical Lidar setled in the front of the robot (see figure 1). Four areas are considered to detect the presence of vegetation, corresponding to the action zone of each nozzle. The figure 5 illustrates these areas of interest. As highlighted on this figure, only the points belonging to each area are

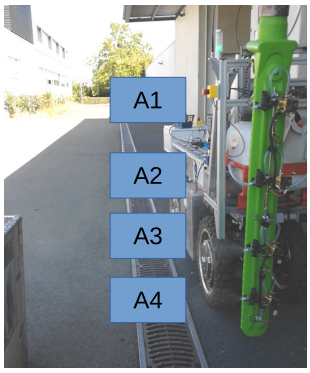

Fig. 5. Areas considered for spraying activation.

considered in the points cloud supplied by the vertical Lidar. If there is a sufficient number of points $N^i > N_v^i$ in the i^{th} area ($i \in [1..4]$), then it is considered that vegetation is present and the i^{th} nozzle has to be activated to spray the corresponding vegetation. The threshold N_v^i has to be chosen in order to avoid false detection (due to dust, or light rain, or even droplet coming from spraying and wind). In practice, all the threshold are the same and chosen equal to 10 points. Such a threshold has been chosen experimentally relying on the Lidar properties and has to be adapted to the application and the sensor considered.

B. Predictive layer for delay compensation

The previous detection does not directly control the nozzle, since the Lidar is situated in front of the robot, and nozzles have a settling time τ_N (equal in this case to 0.4s). As a result, a table containing the presence of vegetation with respect to the longitudinal distance $L2$ between the Lidar is on-line updated.

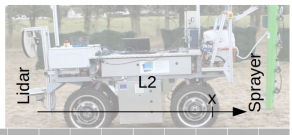

Nozzle 1	1	0	0	0	0	0	1	1	1
Nozzle 2	1	0	0	1	1	1	1	1	1
Nozzle 3	1	1	1	1	1	1	1	1	1
Nozzle 1	1	1	1	0	0	0	1	1	1

Fig. 6. Illustration of the table containing the presence of the vegetation along the robot length.

Figure 6 illustrates such a table, storing the presence of the vegetation along the length of the robot. Thanks to such a table, one can synchronize the presence of the vegetation in front of each nozzle, despite the position of the Lidar in front of the robot. As a result, one can also predict the future presence of the vegetation for each nozzle, knowing the actuator delay. As a result, the table is shifted from the distance corresponding to this delay knowing the speed: $d = v\tau$.

By denoting $\mu^i(x) \in \{0,1\}$ the presence of any vegetation in the area i at the longitudinal distance x from the vertical lidar, one can then defined the binary control of the i^{th} nozzle

by the following law:

$$N^i = \begin{cases} \mu^i(L_2 - v\tau) & \text{if } |v| > vlim \\ 0 & \text{else} \end{cases}, \quad (14)$$

where $vlim$ is a threshold on the velocity allowing to stop spraying when the robot does not move.
This control allows the synchronization of each nozzle of the sprayer with respect to the robot motion, and the presence of the vegetation.

V. Experimental results

A. Description of experiment

Figure 7 depicts the experimental testbed used to test the proposed approach of autonomous spraying robot in a known case. The robot has indeed to follow the artificial hedge of $12m$ length, installed in a straight line configuration. Four successive areas of hedge have been set on the ground, each separated by $0.5m$, $0.5m$ and $1m$. The first three areas have an height of $1.2m$, while the last one is only $1m$ height, allowing to observed the separation in the activation of each nozzle. After the hedge part, some stakes are still present in order

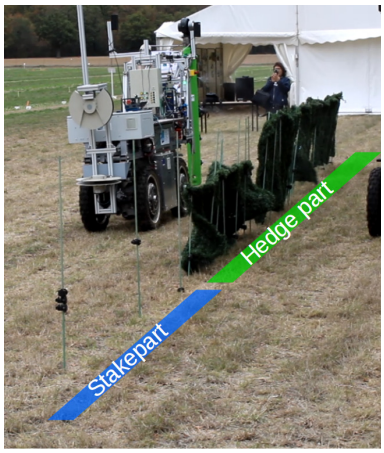

Fig. 7. Environment of experimentation for autonomous spraying.

to install some more artificial vegetation. This latter may be detected and followed by the robot, even if containing only few points in the Lidar detection. One will see in the forthcoming sections that the edge detection in this area is nevertheless difficult.
The robot has to follow this hedge at a desired distance of $1m$, and at a velocity of $0.8m.s^{-1}$. A video of this experiment, with a second robot following the first one used for other development, is available on the link below[1]. A total of 10 following have been achieved showing approximatively the same results detailed in the following. On the video, once the structure is no more detected, the robot can be either remotely controlled, or follow a trajectory thanks to RTK-GPS.

[1]https://stratus.irstea.fr/f/6d0307fbd3344070a490/?dl=1

B. Edge following results

Figure 8 depicts the lateral deviation e_y with respect to the achieve distance. One can notice that after the convergence distance (tuned to $2m$ thanks to the parameter k_d), the lateral deviation stays close to zero (within $\pm 10cm$, which is the expected accuracy of positioning for this kind of application). One can notice that at the end of the hedge part (achieved

Fig. 8. Lateral deviation recorder during the test.

distance of $11m$), an instantaneous deviation of $1.25m$ is recorded, due to a detection of a structure on the right of the robot (coming from surrounding pedestrians). Indeed, after the edge, the only detectable structure is the thin stakes that are supposed to held the artificial hedge. As a result, the robot starts following a wrong structure until it detects an edge from the stakes. The lateral deviation then suddenly goes back to zero (at an achieved distance of $13m$), and stays close to zero. Nevertheless, one can see that the accuracy is deprecated, since the edge detection is disturbed by the few points detected on the stakes. This also causes the stop of the robot that can be noticed on the video, occurring when the trajectory is not available. As a result, in order to be efficient, the edge following has logically to be run on a structure able to supply a sufficiently high number of points enabling the detection of a relevant trajectory.

C. Spraying adaptation results

Once the robot is able to be accurately control with respect to a structure, the autonomous control for the sprayer may be proceed. During the hedge following, the differentiate control of each nozzle is reported on the figure 9.

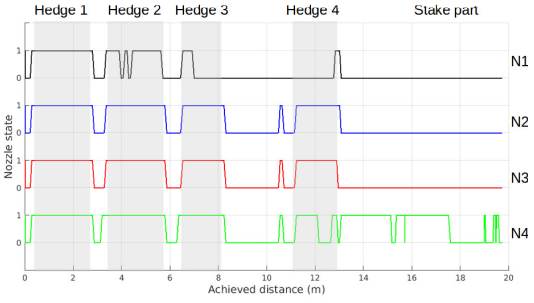

Fig. 9. Results related to nozzles control.

This figure depicts the control state for each nozzle i, $i \in \{1,2,3,4\}$ with respect to the achieved distance. One can easily see the four parts of hedge (between 0-$2.5m$, 3.5 to $5.5m$, 6.5 to $8m$ and 11 to $13m$). As it can be seen, when the sprayer is in front of hedges 1 and 2 the four nozzles are activated, since the height of vegetation covers the four

areas of interest (A_1 to A_4 defined on the figure 5). When the sprayer is in front of hedges 3 and 4, the height of vegetation is lower (especially for hedge 4). As a result, the first nozzle (N1) is not activated (or just punctually because the height of vegetation is borderline the area of interest A_1). Other nozzles stay well activated during these periods (hedge 3 and hedge 4). Between hedges, the absence of vegetation leads to a closure of all nozzles, showing the adaptation of the spraying with respect to the vegetation detection.

The end of hedge area may also be identified on the figure 9, occuring at $13m$. This is in line with the end of the structure detection for the robot motion control, occurring at $11m$ on the figure 8, since the distance L_2, is equal to $2m$. During the stake part, all the nozzles from i=1 to 3 are logically set to off, since the stakes do not generate a sufficient number of points (N_v^i) in the areas of interest A_i. Nevertheless, the lower nozzle 4 is activated. This is due to the yaw angle of the robot, which is neglected in this paper, and the ground then generates points in the region of interest A_4. This drawback may be addressed by considering the soil, thanks to a profile detection, or geometrical computation using the measurement of the robot's yaw angle.

VI. CONCLUSIONS

This paper proposes a control architecture for the autonomous and accurate spraying using an off-road mobile robot in the framework of Precision Farming. An automated sprayer using four independent nozzles has been developed in order to adapt the use of product to the vegetation covering. The cut-off of each nozzle is achieved thanks to a Lidar based on the front of the robot, and the synchronization with the robot motion. This latter action is ensured thanks to a control law based on the detection of edge using a second horizontal Lidar. The efficiency of the proposed control architecture has been tested through full scale experiments, using artificial hedge, with different heights. Results show the accuracy of the robot positioning with respect to the vegetation row, as well as the adaptation of the nozzles state with respect to the vegetation coverage.

In order to go further in the evaluation of the efficiency of this control architecture, more experiments measuring the spraying efficiency are expected to be done with specific test bench. Moreover, it can be seen that the control of the lower nozzle is subjected to perturbations due to the soil detection because of the lateral inclination of the robot. As a result a correction of this drawback using the estimation of the whole robot state (roll and pitch) is under development. The accurate control of spraying tool using additional degree of freedom (using a manipulator arm for instance), is also a way of develoment to ensure a more accurate relative position an orientation of the sprayer with respect to the vegetation.

One of the main limitation of the strategy presented in this paper lies in the fact that two lidars are used. On going works are investigating the possibility of using a single sensor to achieve both the motion control and the measurement of the vegetation covering. Beyond the use of 3D lidar (such as Velodyne), the development of specific sensors based on vision is under studies. An additional benefit of such a three-dimensional sensor also lies in the reconstruction of 3D-mapping allowing to analysis the cross-ability of the area in front of the robot and then avoid obstacles. The safety aspect is indeed a mandatory condition in order to deploy such a solution, allowing to limit environmental impact of agriculture activities, while preserving the level of production to feed the worldwide population.

ACKNOWLEDGMENT

This work receives the financial support of CCMSA[2]. It has also been sponsored by the French government research program "Investissements d'Avenir" through the IDEX-ISITE initiative 16-IDEX-0001 (CAP 20-25), the IMobS3 Laboratory of Excellence (ANR-10-LABX-16-01) and the RobotEx Equipment of Excellence (ANR-10-EQPX-44). This research was also financed by the European Union through the Regional Competitiveness and Employment program -2014-2020- (ERDF - AURA region) and by the AURA region.

REFERENCES

[1] E. Crist, C. Mora, and R. Engelman, "The interaction of human population, food production, and biodiversity protection," *Science*, vol. 356, no. 6335, pp. 260–264, 2017.

[2] T. W. Griffin and E. A. Yeager, "Adoption of precision agriculture technology: A duration analysis," in *In Proceedings of 14th International Conference on Precision Agriculture. Monticello, IL: International Society of Precision Agriculture*, 2018.

[3] S. Blackmore, "Towards robotic agriculture," in *SPIE Commercial+ Scientific Sensing and Imaging*. International Society for Optics and Photonics, 2016, pp. 986 603–986 603.

[4] M. Bergerman, J. Billingsley, J. Reid, and E. Van Henten, "Robotics in Agriculture and Forestry," in *Springer Handbook of Robotics*. Springer International Publishing, 2016, pp. 1463–1492.

[5] R. Saddem-Yagoubi, O. Naud, P. Cazenave, K. Godary-Dejean, and D. Crestani, "Precision spraying: from map to control using model-checking," 2017.

[6] P. Mehta, "Automation in agriculture: agribot the next generation weed detection and herbicide sprayera review," *J. Basis Appl. Eng. Res*, vol. 3, no. 3, pp. 234–238, 2016.

[7] C. Penn *et al.*, "Twelve innovations from vinitech 2018," *Australian and New Zealand Grapegrower and Winemaker*, no. 660, p. 56, 2019.

[8] G. Bayar, M. Bergerman, A. B. Koku, and E. I. Konukseven, "Localization and control of an autonomous orchard vehicle," *Computers and Electronics in Agriculture*, vol. 115, pp. 118 – 128, 2015. [Online]. Available: http://www.sciencedirect.com/science/article/pii/S0168169915001519

[9] M. Bastianelli, V. De Rudnicki, S. Codis, X. Ribeyrolles, and O. Naud, "Two vegetation indicators from 2d ground lidar scanner compared for predicting spraying deposits on grapevine," 2017.

[10] J. Cheng, B. Wang, Y. Xu, and K. Wang, "Construction method of line-segments based map from 2D laser sensor data for mobile robot," in *36th Chinese Control Conference (CCC)*, 2017, pp. 5849–5852.

[11] P. Skrzypczynski, "Building geometrical map of environment using IR range finder data," in *Proc. Conf. Intelligent Autonomous Systems 4, Karslruhe*, 1995, pp. 408–412.

[12] V. Nguyen, A. Martinelli, N. Tomatis, and R. Siegwart, "A comparison of line extraction algorithms using 2D laser rangefinder for indoor mobile robotics," in *IEEE/RSJ International Conference on Intelligent Robots and Systems*, 2005, pp. 1929–1934.

[13] A. Harati and R. Siegwart, "A new approach to segmentation of 2D range scans into linear regions," in *IEEE/RSJ International Conference on Intelligent Robots and Systems*, 2007, pp. 2083–2088.

[14] C. Samson, P. Morin, and R. Lenain, "Modeling and control of wheeled mobile robots," in *Springer Handbook of Robotics*. Springer, 2016, pp. 1235–1266.

[15] M. Deremetz, A. Couvent, R. Lenain, B. Thuilot, and C. Cariou, "A generic control framework for mobile robots edge following," *Lecture Notes in Electrical Engineering*, vol. 613, 2019.

[2]French Social Insurance for Agriculture Workers